

Evidence for an Energy Scale for Quasiparticle Dispersion in $\text{Bi}_2\text{Sr}_2\text{CaCu}_2\text{O}_8$

P. V. Bogdanov,¹ A. Lanzara,^{1,2} S. A. Kellar,¹ X. J. Zhou,¹ E. D. Lu,² W. J. Zheng,¹ G. Gu,³ J.-I. Shimoyama,⁴ K. Kishio,⁴ H. Ikeda,⁵ R. Yoshizaki,⁵ Z. Hussain,² and Z. X. Shen¹

¹*Department of Physics, Applied Physics and Stanford Synchrotron Radiation Laboratory, Stanford University, Stanford, California 94305*

²*Advanced Light Source, Lawrence Berkeley National Laboratory, Berkeley, California 94720*

³*School of Physics, University of New South Wales, P.O. Box 1, Kensington, New South Wales, Australia 2033*

⁴*Department of Applied Chemistry, University of Tokyo, Tokyo, 113-8656, Japan*

⁵*Institute of Applied and Cryogenic Center, University of Tsukuba, Tsukuba, Ibaraki 305, Japan*

(Received 20 December 1999)

Quasiparticle dispersion in $\text{Bi}_2\text{Sr}_2\text{CaCu}_2\text{O}_8$ is investigated with improved angular resolution as a function of temperature and doping. Unlike the linear dispersion predicted by the band calculation, the data show a sharp break in dispersion at 50 ± 15 meV binding energy where the velocity changes by a factor of 2 or more. This change provides an energy scale in the quasiparticle self-energy. This break in dispersion is evident at and away from the d -wave node line, but the magnitude of the dispersion change decreases with temperature and with increasing doping.

PACS numbers: 74.62.-c, 74.72.Hs

In a conventional metal the observation of an energy scale often provides significant insight into the physical process in the material. The most noted example is the observation of the phonon anomalies in strong coupling superconductors such as lead, which had a far-reaching impact on the understanding of the superconductivity mechanism [1–3]. For the high-temperature superconductors, a peculiar normal state property is the fact that there appears to be no energy scale, which is often referred to as the marginal Fermi liquid behavior [4]. This behavior is highly anomalous as one would expect certain energy scales in the problem, say, phonons which are obviously present in the crystal. In the theoretical context this lack of an energy scale is believed to be a key feature of a nearby quantum critical point [5]. In the superconducting state, on the other hand, there are energy scales observed in the cuprate superconductors, such as the superconducting gap.

With its ability to measure both the real and imaginary parts of the self-energy, $\Sigma(\omega, k)$, angle-resolved photoemission (ARPES) experiments provide a unique opportunity to further explore this issue as any relevant energy scale present will manifest itself in the quasiparticle dynamics. In the known case of electron-phonon interaction the coupling causes a kink in the dispersion and also a change in quasiparticle lifetime near the phonon energy [3]. These canonical changes reveal effects in the real and imaginary parts of the self-energy due to the electron-phonon interaction, an effect which is experimentally observed recently [6]. In this Letter, we present high-resolution ARPES data from $\text{Bi}_2\text{Sr}_2\text{CaCu}_2\text{O}_8$ superconductors as a function of doping and temperature. We have observed a clear break in the quasiparticle dispersion near 50 ± 15 meV binding energy (BE) that results in a change in the quasiparticle velocity up to a factor of 2 or more. This effect is enhanced in the underdoped sample, and appears to persist above T_C where the break

becomes rather broad. Because the electronic structure calculation [7] predicts a linear dispersion in this range, this result represents an important effect in the real part of the self-energy with a scale near 50 ± 15 meV. Further, we found that this effect is present at various points of the momentum space. We believe the doping, temperature, and k -dependent information presented here will put a constraint on microscopic theory.

Angle-resolved photoemission data have been recorded at beam line 10.0.1.1 of the Advanced Light Source utilizing 22, 33, and 55 eV photon energies, in a similar setup as we have reported recently [8]. The momentum resolution was $\pm 0.1^\circ$, which is about an order of magnitude better than our previous study of this material, making the results reported in this Letter possible. The energy resolution was 14 meV. The vacuum during the measurement was better than 4×10^{-11} torr. The underdoped (UD) $\text{Bi}_2\text{Sr}_2\text{CaCu}_2\text{O}_8$ ($T_C = 84$ K) and the slightly overdoped (OD) $\text{Bi}_2\text{Sr}_2\text{CaCu}_2\text{O}_8$ samples ($T_C = 91$ K) were grown using the floating-zone method. The single crystalline samples were oriented and cleaved *in situ* at low temperature.

Figure 1(a) shows raw ARPES data collected along the $(0, 0)$ to (π, π) (nodal) direction of the Brillouin zone (BZ) from the OD sample at 30 K. In Fig. 1(b) we plot the dispersion determined from the fits to the momentum distribution curves (MDCs)—angle scans at a constant binding energy [9]. MDC plots show a peak on a constant background that can be fitted very well with a simple Lorentzian, as illustrated in the inset (b2) of Fig. 1. Error bars in k_{\parallel} and energy are determined from the fit uncertainty and energy resolution, respectively. The data clearly show a feature dispersing towards the Fermi energy with an obvious break in the slope near 50 meV BE. A similar break in the dispersion was also observed at photon energies 22 and 55 eV. Data for all three photon energies

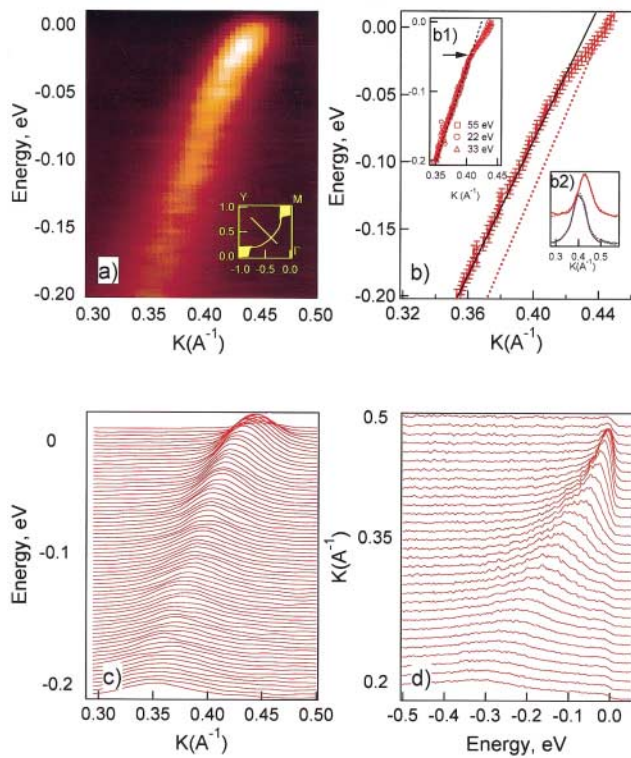


FIG. 1 (color). Panel (a) shows raw data obtained using Scienta angle mode for slightly overdoped ($T_c = 91$ K) $\text{Bi}_2\text{Sr}_2\text{CaCu}_2\text{O}_8$ along nodal direction (Γ - Y) of the BZ at 33 eV photon energy. The position of the cut is given in the inset. Panel (b) shows the dispersion of the quasiparticle determined from the MDC fits of the data in panel (a). The theoretical dispersion from LDA calculation is also included (dotted straight line). Energy is given relative to the Fermi energy. Inset (b1) shows the dispersion along this direction obtained at 22, 33, and 55 eV. Inset (b2) shows MDC's at 16 (blue) and 55 (red) meV BE. Dashed lines represent Lorentzian fits. Panels (c) and (d) show raw MDCs and EDCs, respectively.

are plotted in the inset (b1) of Fig. 1. To describe the dispersion in the range of (-200 to 0 meV) one needs only two straight lines intersecting near 50 meV BE. This behavior is clearly different from what one expects from the local density approximation (LDA) or any other electronic structure calculation where a linear dispersion in this energy range is predicted. Raw MDCs are plotted in panel Fig. 1(c), while raw energy distribution curves (EDCs) are plotted in Fig. 1(d) for reference.

We present in Figs. 2(a)–2(c) the dispersions obtained from different cuts parallel to the $(0, 0)$ to (π, π) direction across the Fermi surface for the UD sample at 20 K. Within the error bars, the data are again well described by two straight lines with a break near 50 meV BE. The energy position of the break is constant throughout the BZ within the experimental uncertainty, despite the opening of the gap. Figure 3 shows the locations in the two-dimensional zone where the break is experimentally observed. It demonstrates that the effect is present in all directions.

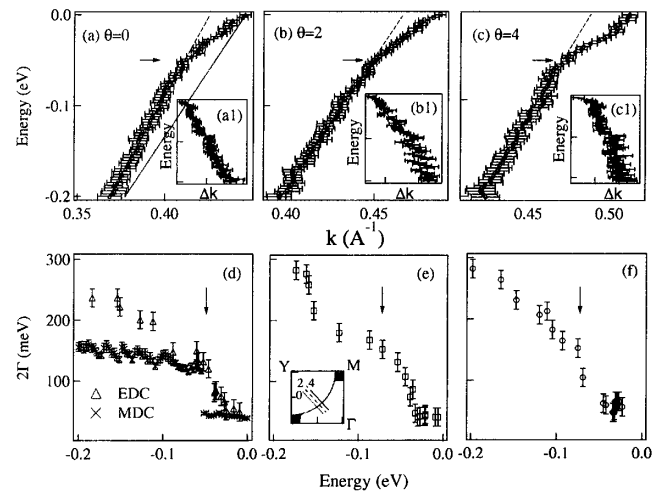


FIG. 2. Panels (a) to (c) show the MDC-derived dispersions for the underdoped $\text{Bi}_2\text{Sr}_2\text{CaCu}_2\text{O}_8$ ($T_c = 84$ K) for cuts parallel to the Γ - Y direction vs the momentum. [The positions of the cuts in the BZ are shown in the inset of (e).] The linear fits to the dispersions are also shown. Insets (a1) to (c1) show MDC derived quasiparticle widths in momentum space along the cuts as a function of binding energy. Panels (e) and (f) show EDC derived quasiparticle widths in energy space along the cuts as a function of binding energy. Panel (d) shows EDC width together with the peak width in energy space derived from MDC of inset (a1) via velocity determined from dispersion of panel (a). Energy is given relative to Fermi energy.

We have investigated this effect as a function of doping and temperature. The effect appears to be stronger in the underdoped sample. The change of the quasiparticle velocity at the break is different, which can be

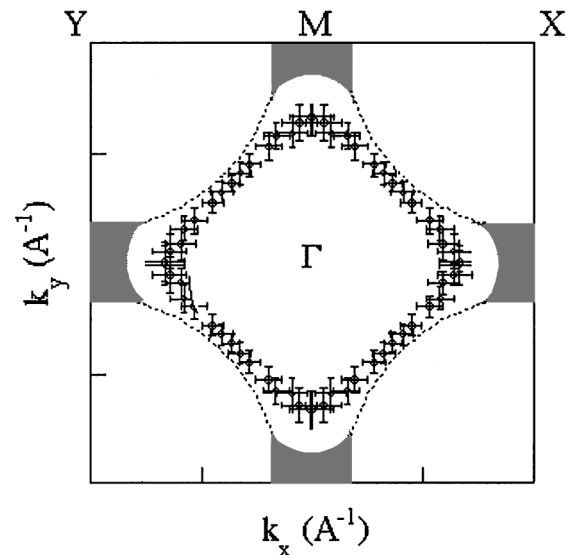


FIG. 3. Kink position as a function of \vec{k}_x and \vec{k}_y is plotted in the BZ (circles). Eightfold symmetrization procedure was applied. Error bars reflect uncertainty in kink position from the MDC fits and the experimental angular resolution perpendicular to the scan direction. Fermi surface is plotted for reference (dashed lines).

illustrated by data along the $(0, 0)$ to (π, π) direction. For the underdoped sample, the quasiparticle velocity determined from the MDC fits shows a break from 3.6 eV \AA at higher binding energies to 1.5 eV \AA near the Fermi level. The respective velocities for the optimally doped samples are 2.6 and 1.6 eV \AA . The error in velocities from the fits is $\pm 0.1 \text{ eV \AA}$ [10].

In general, one expects to see complementary effects in dispersion and EDC and MDC peak widths as they reflect the quasiparticle self-energy. The self-energy can be easily extracted from an ARPES experiment if $\text{Im}\Sigma(\vec{k}, E)$ is much smaller than the energy. In high T_c 's extracting the self-energy from ARPES is harder because the EDC peak energy is comparable to the peak width for $E \geq 30 \text{ meV}$ binding energy. However, assuming weak k dependence of the $\text{Im}\Sigma(k, E)$ [4], the deviation of the MDC dispersion from the LDA calculation gives real part of the self-energy and the MDC peak widths represent the imaginary part [11]. Figures 2(a1)–2(c1) shows MDC widths in momentum space along various cuts. The corresponding energy width is given by the momentum width of the MDC peak multiplied by the velocity if the scan direction is along the energy gradient direction. In our geometry this condition is satisfied only along the nodal direction. In Fig. 2(d) we plot the energy width from MDC together with EDC width. The step effect in MDC energy width is due to linear approximation to the dispersion in determining the velocity, and smoother transition is expected for a less dramatic behavior. EDC peak widths do not simply give $\text{Im}\Sigma(\vec{k}, E)$ in the case of broad peaks. Furthermore, EDC data are complicated by energy-dependent background and Fermi cutoff. Nevertheless, the EDC data still indicate a more abrupt change in the width at the energies corresponding to the kink in the dispersion, as shown in Figs. 2(d)–2(f). We feel that the qualitative consistency between MDC and EDC results is sufficient to make the case for the strong self-energy effect in the data.

The dispersions determined from the OD sample above T_c along the $(0, 0)$ to (π, π) (Γ -Y) direction are shown in Fig. 4(a), while the low-temperature dispersions ($T < T_c$) are reported in Fig. 4(b). The dispersions exhibit the same break structure as contrasted to the straight line. The change of dispersion is more difficult to see in the high-temperature data compared to low-temperature data, but a weak residual effect still appears to be present. In Fig. 4(c) we show the temperature dependence of the EDC width. We see a clear change in 2Γ around $50 \pm 15 \text{ meV}$ in the low-temperature data, but the effect is harder to see above T_c , similar to earlier reports [9,12,13].

We now discuss the origin of the strong self-energy effect near $50 \pm 15 \text{ meV}$. The first possibility that comes to mind is the electron-phonon interaction as there are phonons of this energy scale in the compound [11]. This would explain the persistence of the feature throughout the Brillouin zone and the persistence of the feature above the superconducting transition temperature, since phonons are

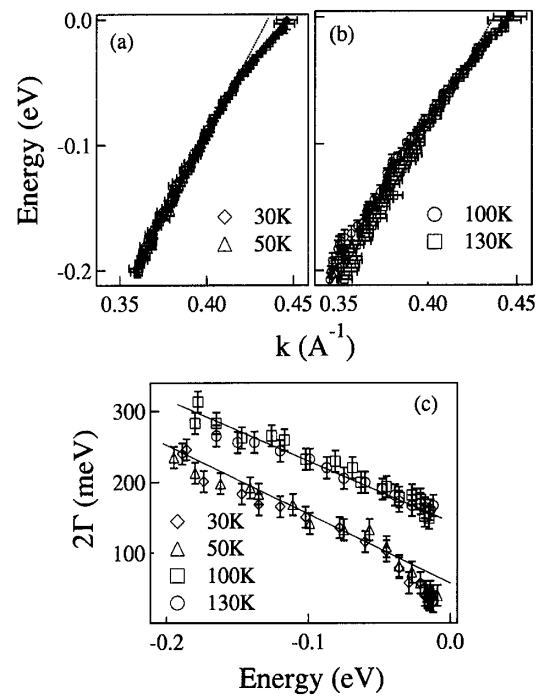


FIG. 4. In panel (a) dispersion in the slightly overdoped $\text{Bi}_2\text{Sr}_2\text{CaCu}_2\text{O}_8$ ($T_c = 91 \text{ K}$) along nodal direction (Γ -Y) of the BZ below T_c is reported. The dotted line represents linear fit into the high energy part of the dispersion. Energy is given relative to Fermi energy. In panel (b) dispersion above T_c is reported for the same sample. The dotted line represents the linear fit into the high energy part of the dispersion. Panel (c) shows EDC derived quasiparticle widths of the spectral feature as a function of binding energy. High-temperature data are shifted up by 100 meV for clarity.

\vec{k} and T independent. However, as shown recently [6], the dispersion tends to recover to the one-electron result when the energy is well above the typical phonon energies, with the total range of the perturbed dispersion below E_F equal to half the Debye temperature. In our case, there is no indication that the dispersion will recover to LDA behavior and the high energy part of the data cannot be fit with a line passing through the Fermi surface crossing. Another problem with the phonon scenario is that it is not a natural explanation on why the effect is stronger in the underdoped sample.

The second possibility is the electron coupling to collective magnetic excitations [15–20]. The energy scale of the resonant neutron mode [21] is consistent with the $50 \pm 15 \text{ meV}$ feature seen in our experiments. This picture is also consistent with the fact that the underdoped sample shows a stronger effect than the overdoped one [21,22]. However, the persistence of the effect above T_c and recent observation of the kink in the $\text{La}_{2-x}\text{Sr}_x\text{CuO}_4$ system [23] are inconsistent with the resonant mode scenario. It may be the kink is a consequence of the electron's coupling to magnetic excitations, while the resonant mode makes the effect particularly strong when it is present. We should note that the coupling of a quasiparticle to collective

excitations was previously discussed, but in a very different context [24,25]. The break in quasiparticle dispersion of an optimally doped sample along the nodal direction is also present in the data of Valla *et al.* [9]. However, authors did not elaborate on this issue, and they suggested the absence of energy scale in the problem.

The third possibility is that we see the effect related to the opening of the superconducting gap which is of the order of 50 ± 15 meV in this compound. Because the antinodal direction near $(\pi, 0)$ has a very high density of states, we expect an effect when this energy scale is reached [26]. The down side of this scenario is the persistence of the effect above T_c .

The last possibility is based on the stripe scenario [8,27–31], where the kink in the dispersion reflects the frequency of the fluctuating stripes or results from the mixing of states from the metallic stripes and insulating domains. As indicated in a recent cluster perturbation calculation, mixing of states from metallic stripes at low binding energy and from insulating domains at higher binding energy leaves a break in dispersion [31].

We thank J.D. Denlinger for the help with the data analysis software. We thank P.D. Johnson, B.O. Wells, S.C. Zhang, D.J. Scalapino, S.A. Kivelson, D.H. Lee, R.B. Laughlin, and P.A. Lee for discussion. The experiment was performed at the Advanced Light Source of Lawrence Berkeley National Laboratory. The Stanford work was supported by an NSF Grant through the Stanford MRSEC grant and NSF Grant No. DMR-9705210. The work at ALS was supported by DOE Office of Basic Energy Science, Division of Materials Science, with Contract No. DE-AC03-76SF00098. The SSRL's work was also supported by the Office's Division of Materials Science.

[1] W.L. MacMillan and J.M. Rowell, in *Superconductivity*, edited by R.D. Parks (M. Dekker Inc., New York, 1969), Vol. 1, Chap. 11, p. 561.
 [2] D.J. Scalapino, J.R. Schrieffer, and J.W. Wilkins, *Phys. Rev.* **148**, 263 (1966).
 [3] D.J. Scalapino, in *Superconductivity* (Ref. [1]), Vol. 1, Chap. 11, p. 561.
 [4] C.M. Varma *et al.*, *Phys. Rev. Lett.* **63**, 1996 (1989).
 [5] S. Chakravarty *et al.*, *Phys. Rev. B* **39**, 2344 (1989); S. Sachdev and J. Ye, *Phys. Rev. Lett.* **69**, 2411 (1992); A. Sokol and D. Pines, *Phys. Rev. Lett.* **71**, 2813 (1993); V.J. Emery and S.A. Kivelson, *Phys. Rev. Lett.* **71**, 3701 (1993); C. Castellani *et al.*, *Phys. Rev. Lett.* **75**, 4650 (1995); C.M. Varma, *Phys. Rev. B* **55**, 14 554 (1997); R.B. Laughlin, *cond-mat/9709195*.

[6] T. Valla *et al.*, *Phys. Rev. Lett.* **83**, 2085 (1999); M. Hengsberger *et al.*, *Phys. Rev. Lett.* **83**, 592 (1999); E. Rottenberg *et al.* (to be published).
 [7] S. Massidda *et al.*, *Physica* (Amsterdam) **152C**, 251 (1988); H. Krakauer and W.E. Pickett, *Phys. Rev. Lett.* **60**, 1665 (1988).
 [8] X.J. Zhou *et al.*, *Science* **286**, 268 (1996).
 [9] T. Valla *et al.*, *Science* **285**, 2110 (1999).
 [10] In Fig. 2 we plot dispersions as a function of angle. The change of velocities with angle is up to 1 eV Å per degree. Although our angular resolution is $\pm 0.1^\circ$, the error in absolute alignment is $\pm 1^\circ$, which is the main source of uncertainty. However, for both dopings we sampled over the whole Brillouin zone. This gives us an internal reference point for alignment, since velocities decrease as we go away from nodal direction. We have measured two overdoped samples at three photon energies. The velocities we determined for both samples for low binding energy part are within 0.1 eV Å. There is no detectable change in velocity with doping or photon energy in this region. Other groups reported 1.14 eV Å [9] and 1.6 eV Å [12] for the low binding energy velocities. For the high energy part the difference with samples is also negligible. For the sample we measured at three photon energies we find 2.6 ± 0.1 eV Å. For a sample of the same doping other experiments gave 2.5 eV Å.
 [11] P.V. Bogdanov *et al.* (unpublished).
 [12] A. Kaminski *et al.*, *Phys. Rev. Lett.* **84**, 1788 (2000).
 [13] A.V. Puchkov *et al.*, *J. Phys. Condens. Matter* **8**, 100049 (1996).
 [14] M.G. Zemlyanov *et al.*, *Sov. Phys. JETP* **77**, 148 (1993); M.G. Zemlyanov *et al.*, *Supercond. Phys. Chem. Technol.* **6**, 435 (1993).
 [15] J. Rossat-Mignod *et al.*, *Physica* (Amsterdam) **235C**, 59 (1994).
 [16] H.F. Fong *et al.*, *Phys. Rev. Lett.* **78**, 713 (1997).
 [17] M. Arai *et al.*, *Phys. Rev. Lett.* **83**, 608 (1999).
 [18] P. Dai *et al.*, *Phys. Rev. Lett.* **77**, 5425 (1996).
 [19] E. Demler and S.-C. Zhang, *Phys. Rev. Lett.* **75**, 4126 (1995).
 [20] P. Dai *et al.*, *Science* **284**, 1344 (1999).
 [21] H.F. Fong *et al.*, *Nature* (London) **398**, 588 (1999).
 [22] H. He *et al.*, *cond-mat/0002013*.
 [23] X.J. Zhou *et al.* (private communication).
 [24] Z.-X. Shen and J.R. Schrieffer, *Phys. Rev. Lett.* **78**, 1771 (1997).
 [25] M.R. Norman *et al.*, *Phys. Rev. Lett.* **79**, 3506 (1997); M.R. Norman and H. Ding, *Phys. Rev. B* **57**, 11 089 (1998).
 [26] A.R. Bishop *et al.*, *Phys. Rev. Lett.* **61**, 2709 (1998).
 [27] V.J. Emery, S.A. Kivelson, and O. Zachar, *Phys. Rev. B* **56**, 6120 (1997).
 [28] J. Zaanen, *J. Phys. Chem. Solids* **59**, 1769 (1998), and references therein.
 [29] J.M. Tranquada *et al.*, *Nature* (London) **375**, 561 (1995).
 [30] A. Bianconi *et al.*, *Phys. Rev. Lett.* **76**, 3412 (1996).
 [31] M.G. Zacher *et al.*, *cond-mat/0005473*.